

## Supporting Information

### Efficient Dimerization of Perfluoroolefin Catalyzed by Strong Nucleophilic Bifunctional Ionic Liquid

Minmin Liu,<sup>ab</sup> Bingxi Song,<sup>bc</sup> Yanhui Hu,<sup>bc</sup> Xianglei Meng,<sup>bc</sup> Renzheng Jiang,<sup>a</sup> Yanyan Diao,\*<sup>bcd</sup> and Yuting Song \*<sup>bc</sup>

<sup>a</sup> School of Chemical Engineering, Shenyang University of Chemical Technology, Shenyang, Liaoning 110142, China

<sup>b</sup> Beijing Key Laboratory of Ionic Liquids Clean Process, Institute of Process Engineering, Chinese Academy of Sciences, Beijing, 100190, China

<sup>c</sup> School of Chemical Engineering, University of Chinese Academy of Sciences, Beijing 100049, China

<sup>d</sup> School of Chemical & Environmental Engineering, China University of Mining and Technology (Beijing), Beijing 100083, P. R. China

\* Corresponding Author: Yanyan Diao, Yuting Song

Tel/Fax: +86-10-82544875, E-mail: yydiao@ipe.ac.cn, yutingsong@ipe.ac.cn.

### Synthesis and Characterization of ILs

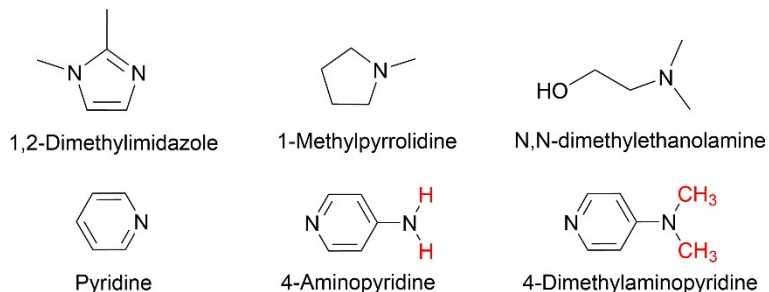
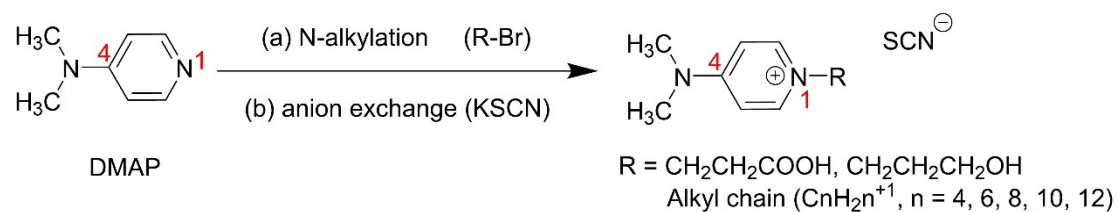


Figure S1. General structures of compound used to synthesize ionic liquids.

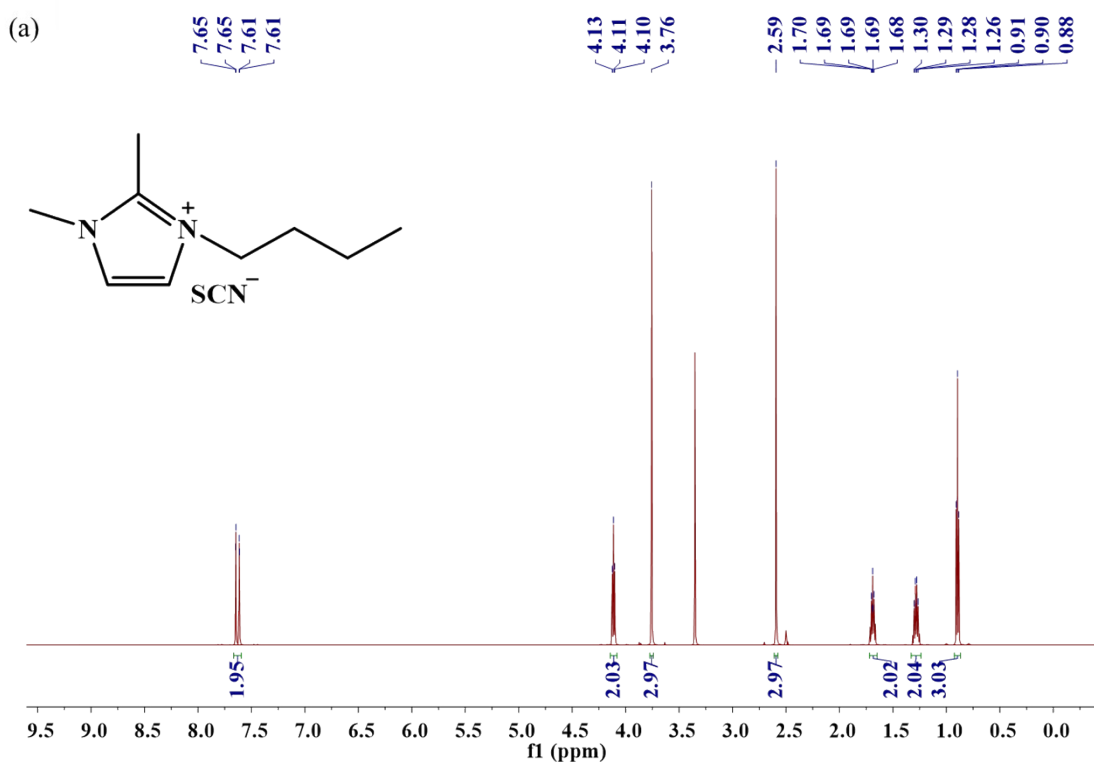


Scheme S1. The synthetic route of DMAP-based thiocyanate ILs

NMR and ESI-MS, as shown in Figure S2-S27, were carried out to identify the structures of the prepared ILs. The results of all catalysts,  $[\text{C}_4\text{Mmim}][\text{SCN}]$ ,

[C<sub>4</sub>Mpyrr][SCN], [P<sub>4,4,4,4</sub>][SCN], [C<sub>4</sub>Py][SCN], [C<sub>4</sub>APy][SCN], [C<sub>4</sub>DMAP][SCN] [C<sub>4</sub>DMEA][SCN], [DMAPPC][SCN], [C<sub>3</sub>OHDMAP][SCN] and [C<sub>n</sub>DMAP][SCN] (n=6, 8, 10, 12) are displayed here. FT-IR and thermogravimetric results of [C<sub>n</sub>DMAP][SCN] ionic liquids are also shown in Figure S28 and S29, respectively.

[C<sub>4</sub>Mmim][SCN]: <sup>1</sup>H NMR (600 MHz, DMSO) δ 7.63 (dd, *J* = 20.7, 2.1 Hz, 2H), 4.11 (t, *J* = 7.3 Hz, 2H), 3.76 (s, 3H), 2.59 (s, 3H), 1.72 – 1.65 (m, 2H), 1.28 (dd, *J* = 15.2, 7.5 Hz, 2H), 0.90 (t, *J* = 7.4 Hz, 3H). <sup>13</sup>C NMR (151 MHz, DMSO) δ 144.19, 129.52, 122.27, 120.84, 47.32, 34.68, 31.19, 18.89, 13.40, 9.19.



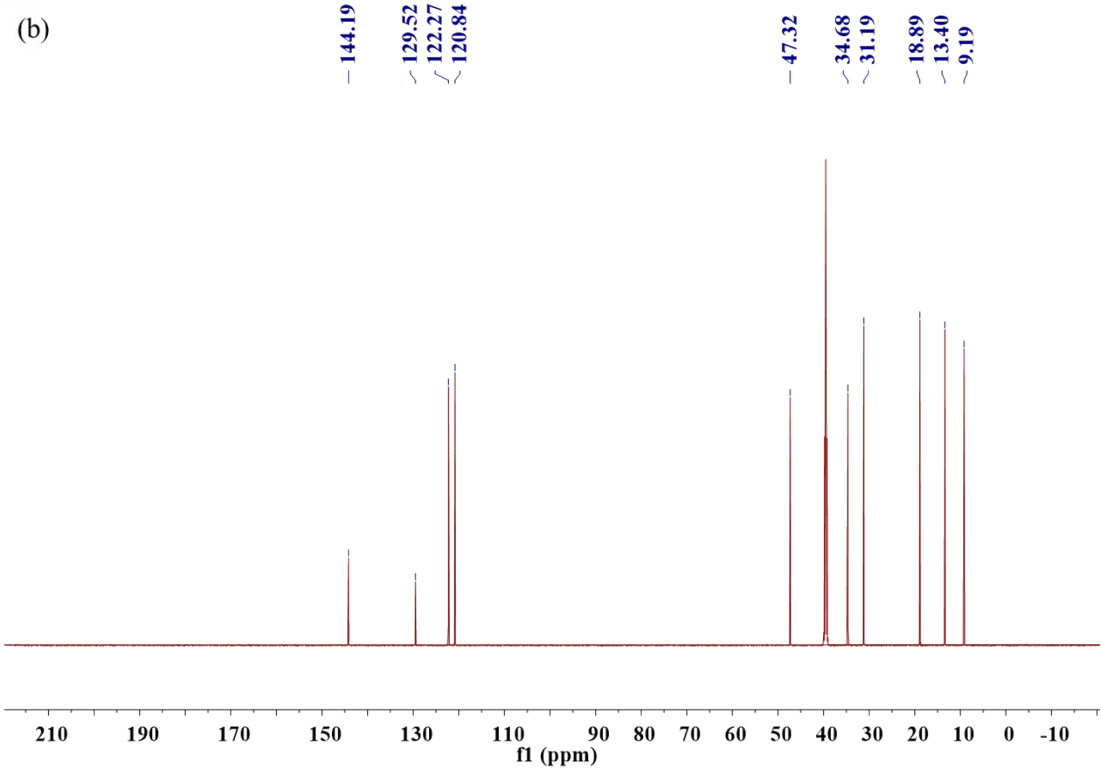


Figure S2. <sup>1</sup>H NMR spectra (a) and <sup>13</sup>C NMR spectra (b) of [C<sub>4</sub>Mmim][SCN].

[C<sub>4</sub>Mpyrr][SCN]: <sup>1</sup>H NMR (600 MHz, DMSO) δ 3.45 (d, J = 23.6 Hz, 4H), 3.32 – 3.28 (m, 2H), 2.99 (s, 3H), 2.08 (s, 4H), 1.68 (s, 2H), 1.32 (dd, J = 14.9, 7.4 Hz, 2H), 0.93 (t, J = 7.4 Hz, 3H). <sup>13</sup>C NMR (151 MHz, DMSO) δ 129.49, 63.43, 63.41, 63.39, 62.90, 47.51, 47.49, 47.46, 24.9, 21.10, 19.31, 13.49.

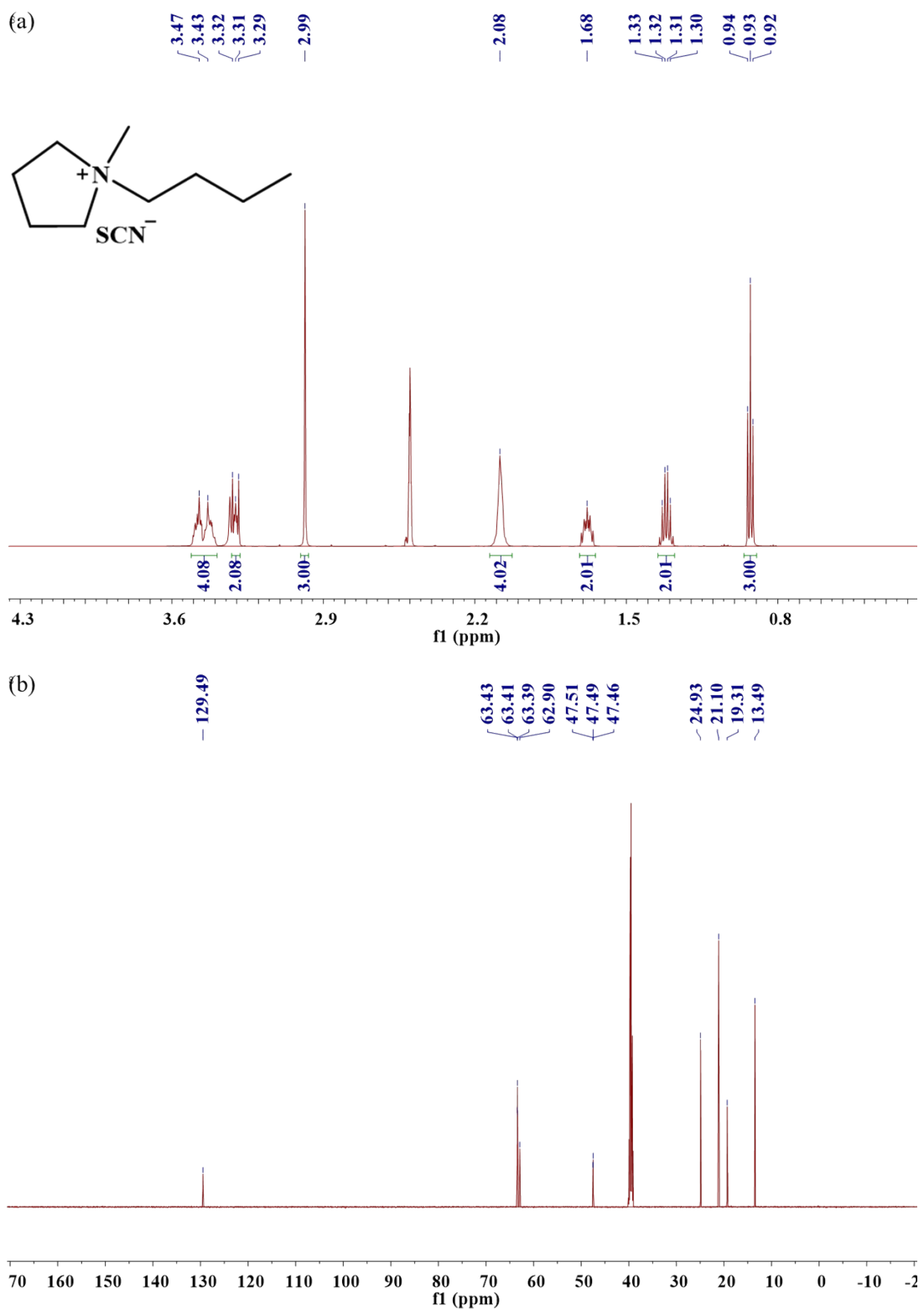


Figure S3.  $^1\text{H}$  NMR spectra (a) and  $^{13}\text{C}$  NMR spectra (b) of  $[\text{C}_4\text{Mpyrr}][\text{SCN}]$ .

[C<sub>4</sub>Py][SCN]: <sup>1</sup>H NMR (600 MHz, DMSO) δ 9.10 (d, *J* = 5.5 Hz, 2H), 8.61 (t, *J* = 7.8 Hz, 1H), 8.17 (t, *J* = 7.0 Hz, 2H), 4.62 (t, *J* = 7.5 Hz, 2H), 1.90 (t, *J* = 7.5 Hz, 2H), 1.29 (dd, *J* = 15.1, 7.5 Hz, 2H), 0.90 (t, *J* = 7.4 Hz, 3H). <sup>13</sup>C NMR (151 MHz, DMSO) δ 145.45, 144.71, 129.58, 128.09, 60.59, 32.64, 18.76, 13.30.

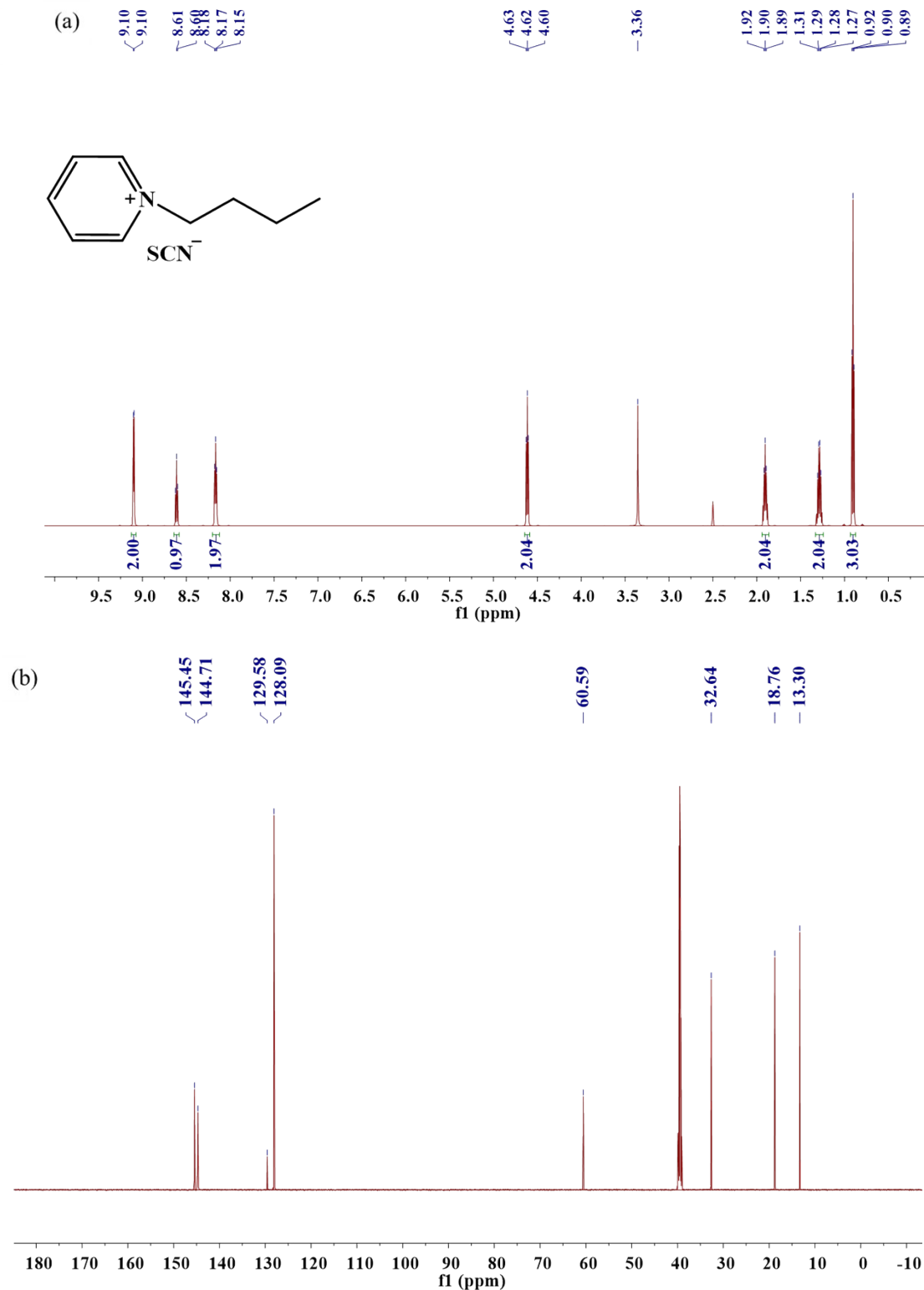
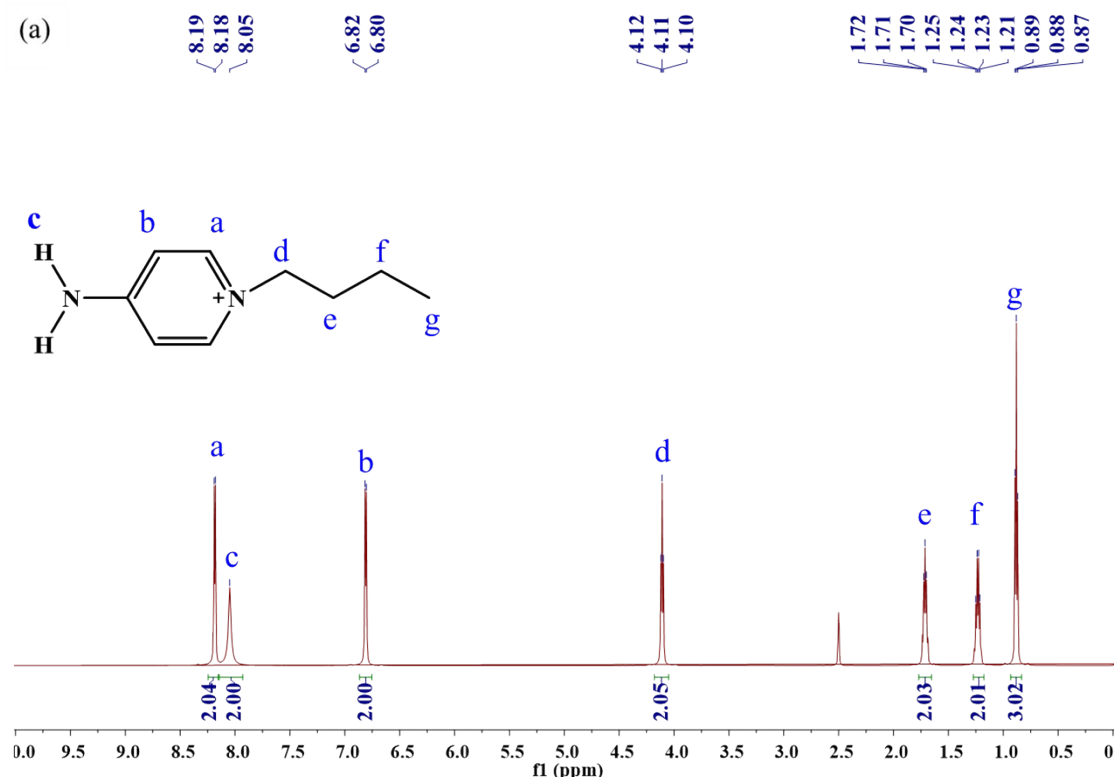


Figure S4.  $^1\text{H}$  NMR spectra (a) and  $^{13}\text{C}$  NMR spectra (b) of [C4Py][SCN].

[C4APy][SCN]:  $^1\text{H}$  NMR (600 MHz, DMSO)  $\delta$  8.18 (d,  $J = 7.1$  Hz, 2H), 8.05 (s, 2H), 6.81 (d,  $J = 7.1$  Hz, 2H), 4.11 (t,  $J = 7.2$  Hz, 2H), 1.77 – 1.65 (m, 2H), 1.23 (dd,  $J = 15.0, 7.4$  Hz, 2H), 0.88 (t,  $J = 7.4$  Hz, 3H).  $^{13}\text{C}$  NMR (151 MHz, DMSO)  $\delta$  158.55, 142.89, 129.74, 109.40, 56.81, 32.25, 18.74, 13.39.



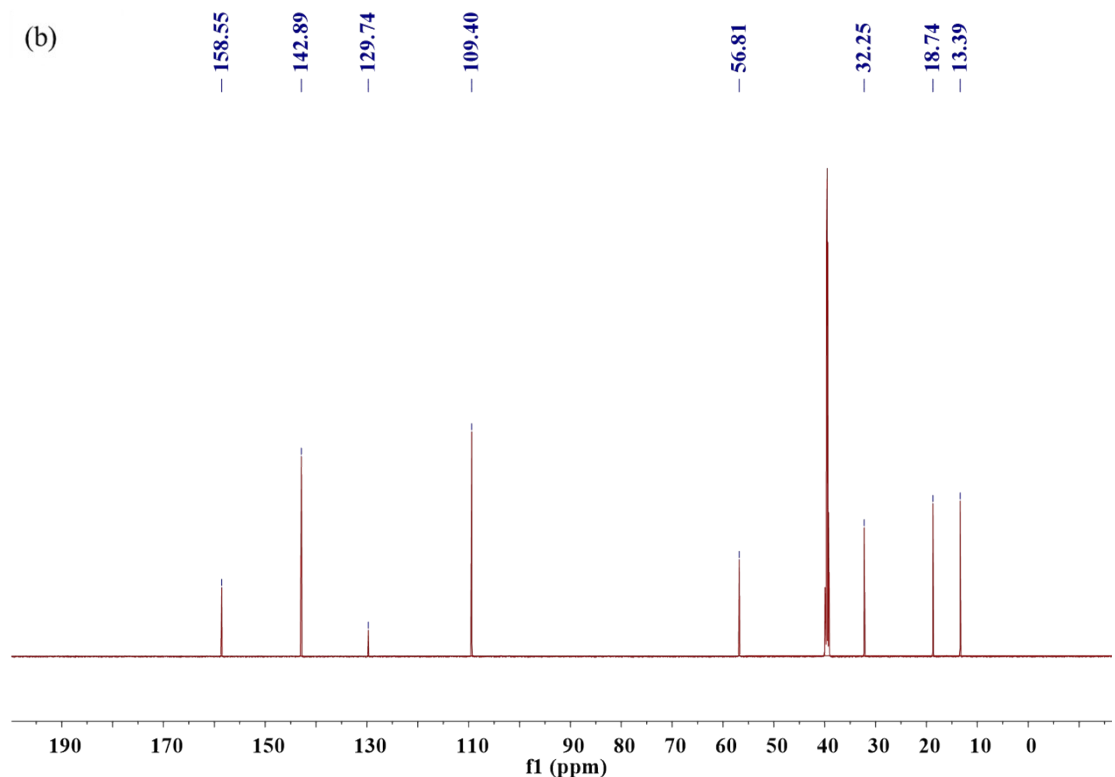


Figure S5. <sup>1</sup>H NMR spectra (a) and <sup>13</sup>C NMR spectra (b) of [C4APy][SCN].

[C<sub>4</sub>DMAP][SCN]: <sup>1</sup>H NMR (600 MHz, DMSO) δ 8.30 (d, *J* = 7.7 Hz, 2H), 7.03 (d, *J* = 7.7 Hz, 2H), 4.16 (t, *J* = 7.2 Hz, 2H), 3.18 (s, 6H), 1.77 – 1.69 (m, 2H), 1.24 (dd, *J* = 15.1, 7.5 Hz, 2H), 0.89 (t, *J* = 7.4 Hz, 3H). <sup>13</sup>C NMR (151 MHz, DMSO) δ 155.82, 141.97, 129.53, 107.68, 56.45, 32.30, 18.73, 13.36.

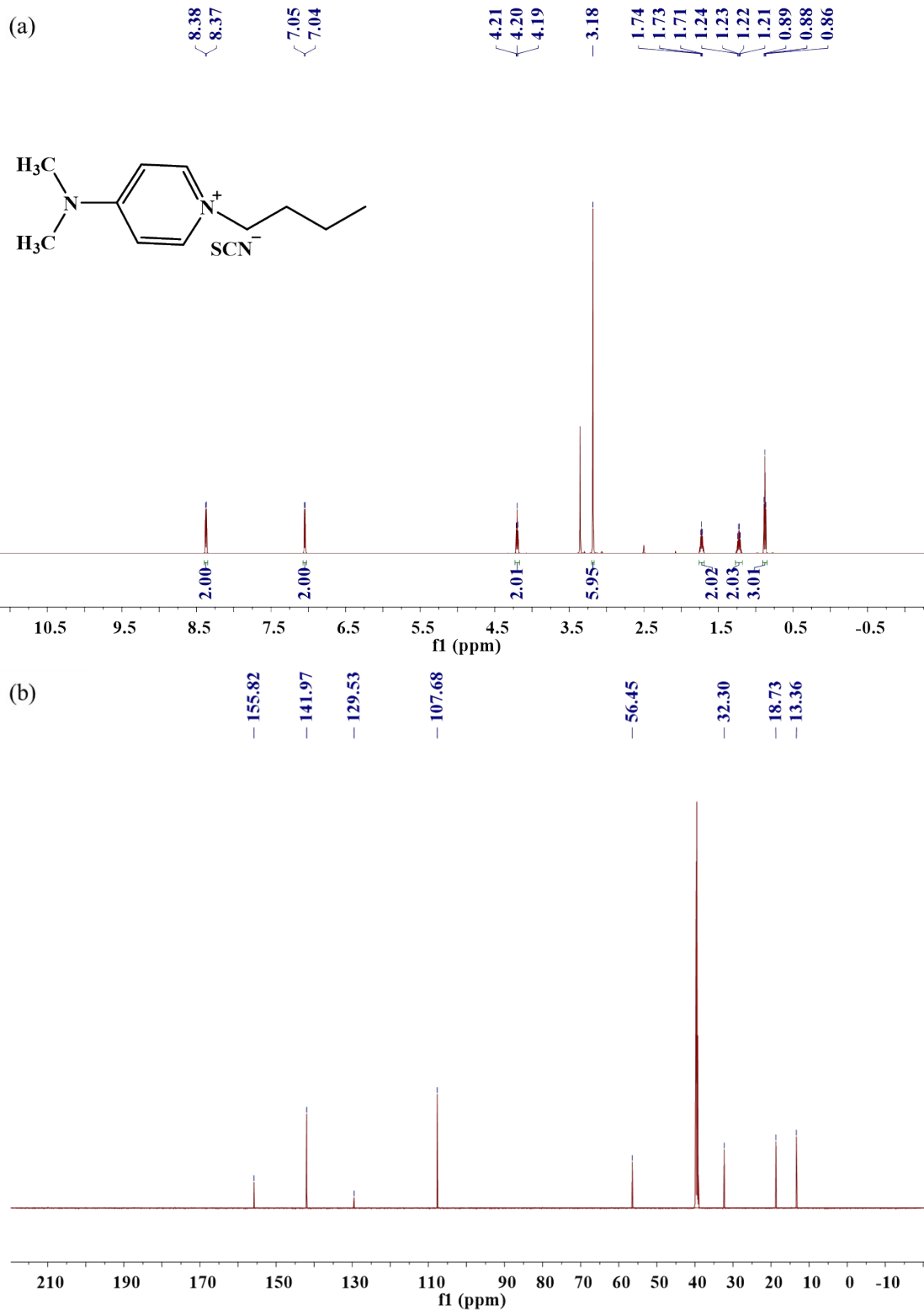


Figure S6.  $^1\text{H}$  NMR spectra (a) and  $^{13}\text{C}$  NMR spectra (b) of [C4DMAP][SCN].

[C<sub>4</sub>DMEA][SCN]:  $^1\text{H}$  NMR (600 MHz, DMSO)  $\delta$  5.25 (s, 1H), 3.81 (s, 2H), 3.34 – 3.30 (m, 2H), 3.06 (s, 6H), 1.66 (s, 2H), 1.29 (dd,  $J$  = 14.8, 7.4 Hz, 2H), 0.92 (t,  $J$  = 7.4 Hz, 3H).  $^{13}\text{C}$  NMR (151 MHz, DMSO)  $\delta$  129.75, 64.61, 63.96, 54.93, 50.84, 50.82,

50.79, 23.80, 19.20, 13.49.

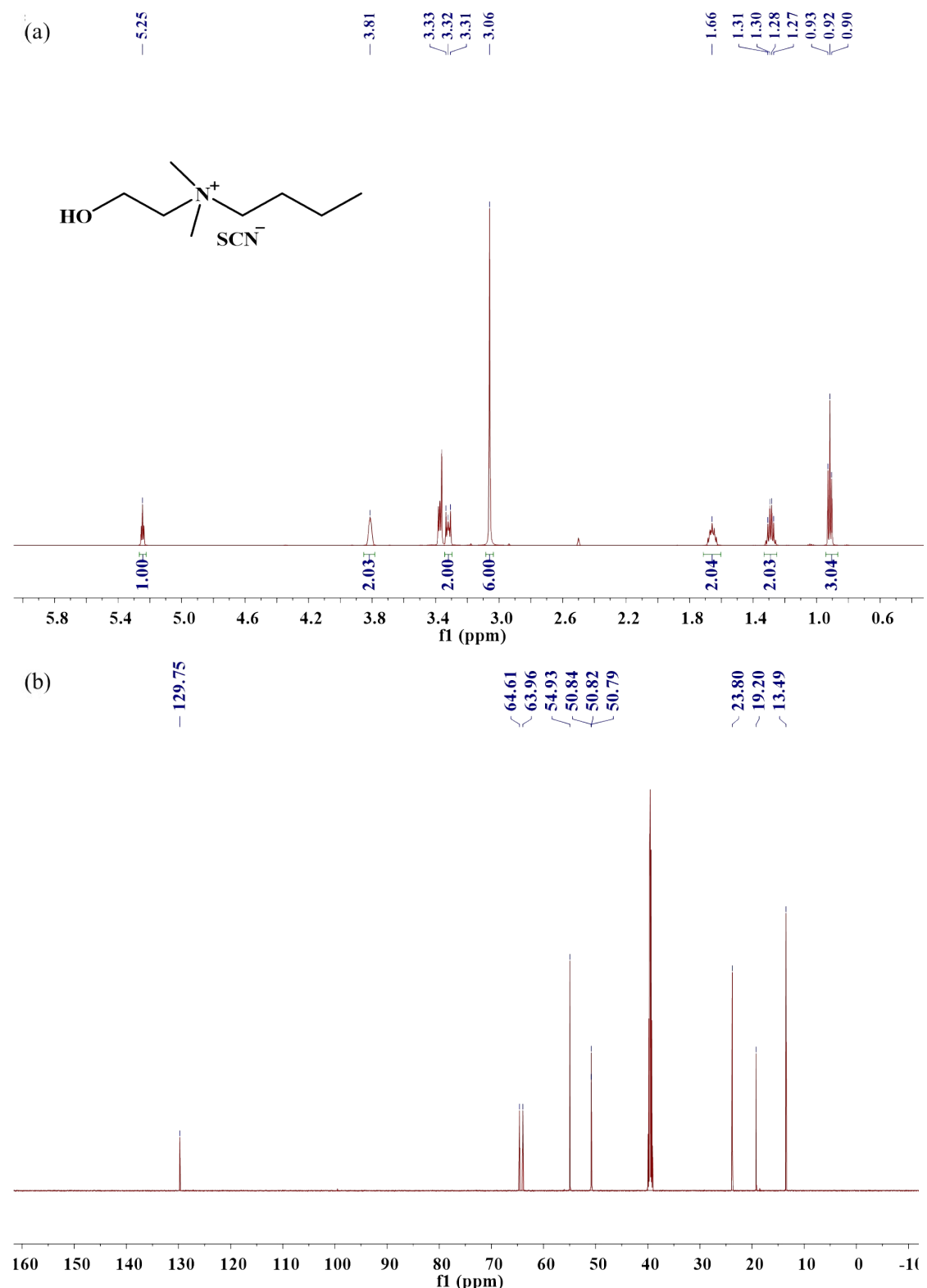


Figure S7.  $^1\text{H}$  NMR spectra (a) and  $^{13}\text{C}$  NMR spectra (b) of [C4DMEA][SCN].

[DMAPPC][SCN]:  $^1\text{H}$  NMR (600 MHz, DMSO)  $\delta$  8.29 (d,  $J = 7.8$  Hz, 1H), 8.21 (d,  $J = 7.6$  Hz, 1H), 7.00 (dd,  $J = 23.4, 7.7$  Hz, 2H), 4.36 (s, 1H), 3.18 (d,  $J = 3.2$  Hz,

8H), 2.88 (s, 1H).  $^{13}\text{C}$  NMR (151 MHz, DMSO)  $\delta$  171.72, 156.94, 155.87, 142.30, 139.06, 129.63, 107.45, 106.97, 52.48, 39.66, 34.44.

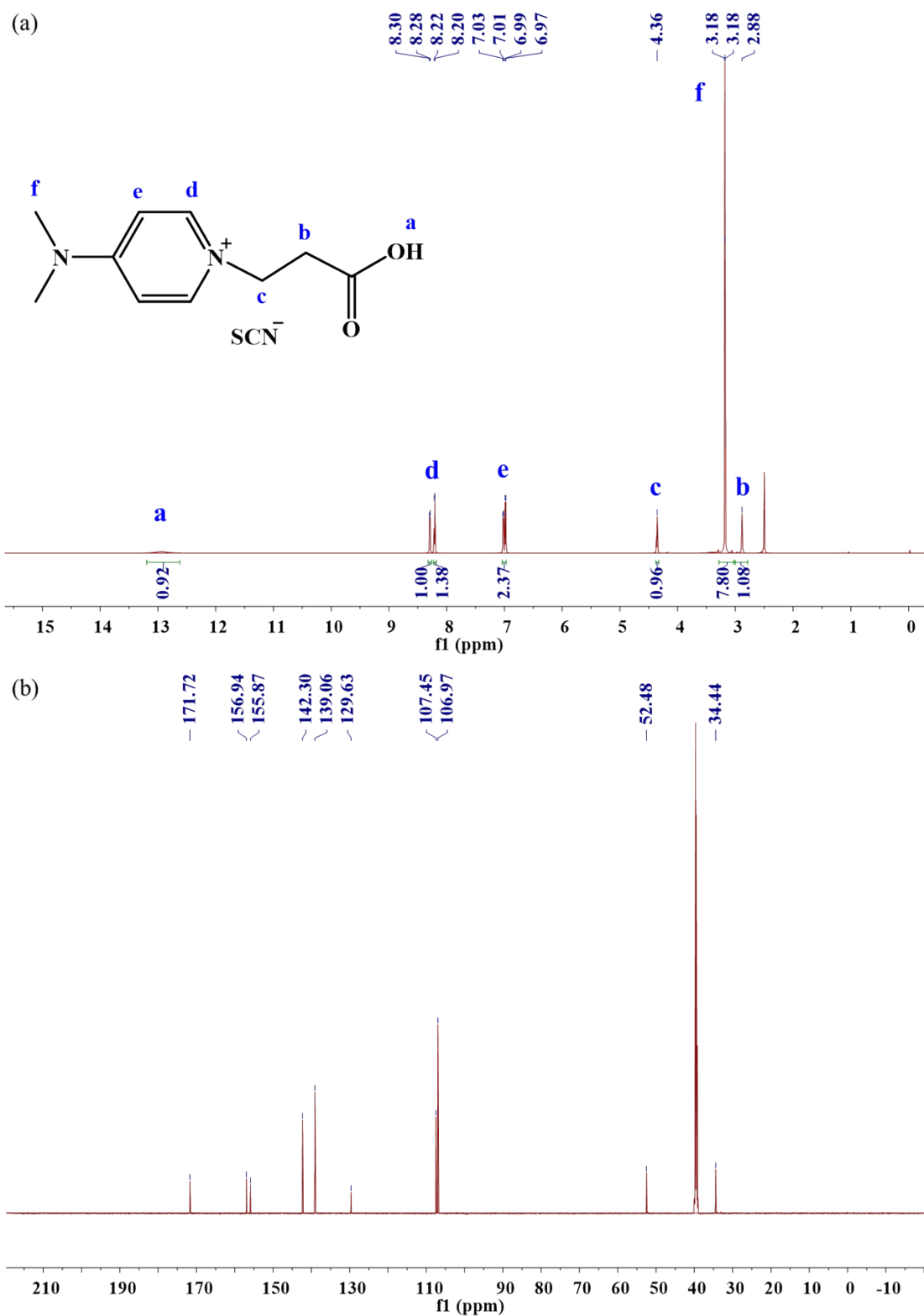


Figure S8.  $^1\text{H}$  NMR spectra (a) and  $^{13}\text{C}$  NMR spectra (b) of [DMAPPC][SCN].

[C<sub>3</sub>OHDMAp][SCN]: <sup>1</sup>H NMR (600 MHz, DMSO) δ 8.26 (d, *J* = 7.8 Hz, 2H), 7.02 (d, *J* = 7.8 Hz, 2H), 4.75 – 4.63 (m, 1H), 4.23 (t, *J* = 7.0 Hz, 2H), 3.38 (s, 2H), 3.18 (d, *J* = 5.2 Hz, 6H), 1.90 (d, *J* = 6.5 Hz, 2H). <sup>13</sup>C NMR (151 MHz, DMSO) δ 155.77 (s), 142.09 (s), 129.74 (s), 107.61 (s), 57.01 (s), 54.26 (s), 39.71 (s), 33.08 (s).

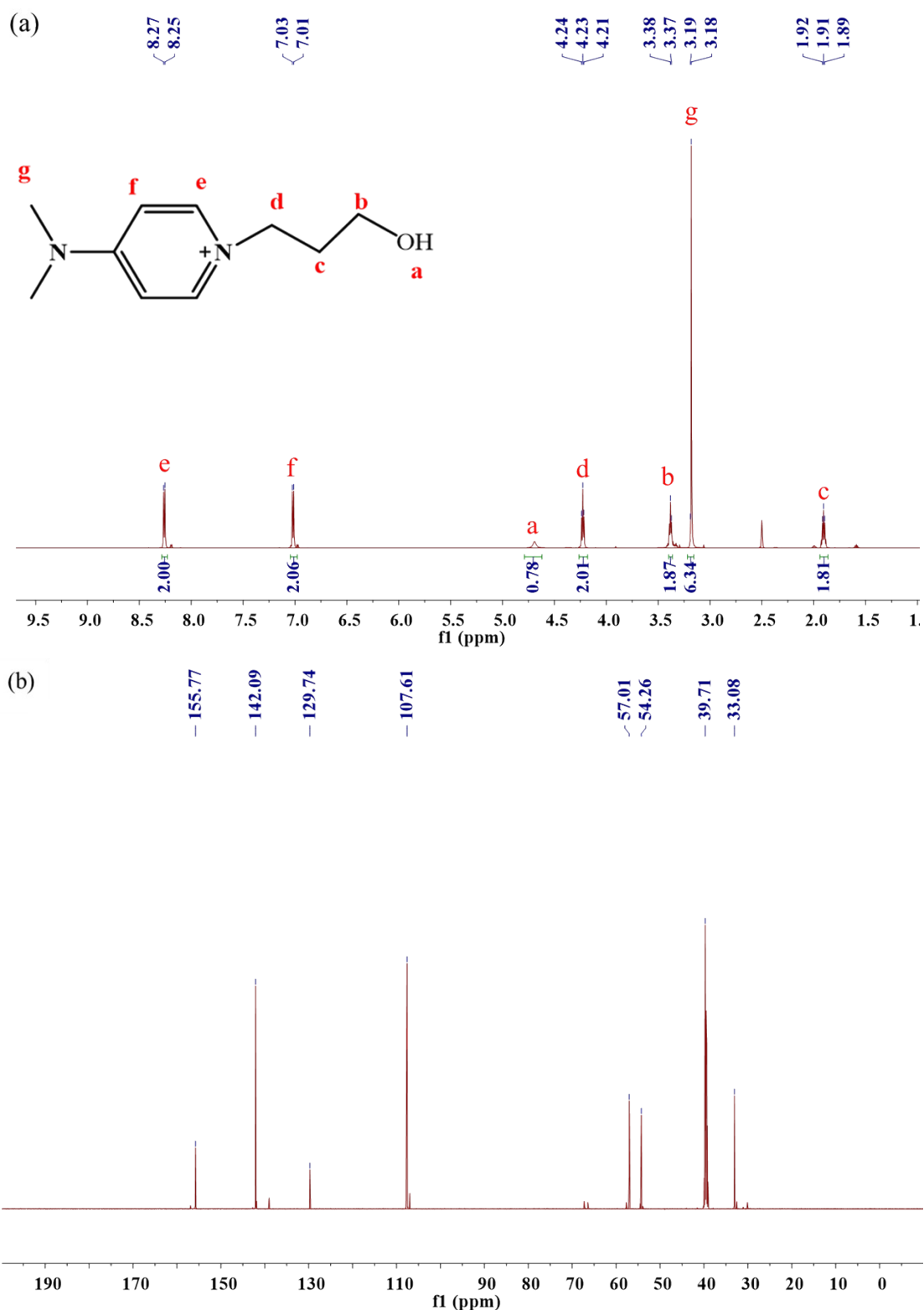
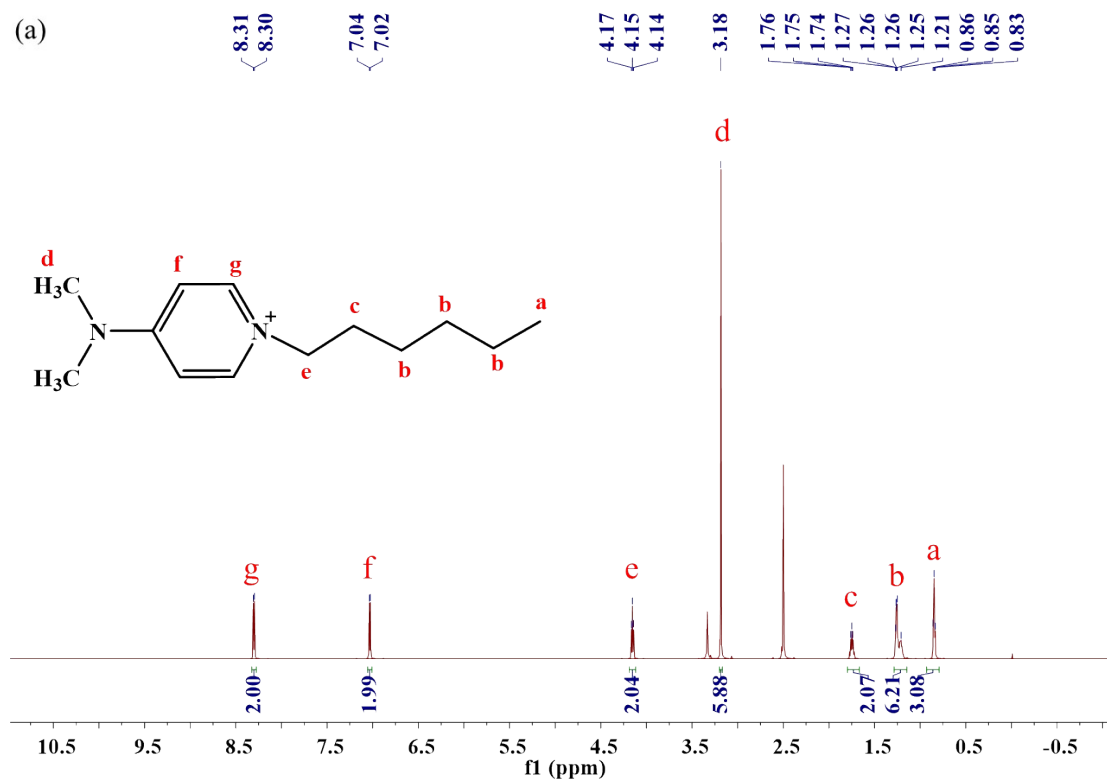


Figure S9  $^1\text{H}$  NMR spectra (a) and  $^{13}\text{C}$  NMR spectra (b) of  $[\text{C}_3\text{OHDMAp}][\text{SCN}]$ .

$[\text{C}_6\text{DMAP}][\text{SCN}]$ :  $^1\text{H}$  NMR (600 MHz, DMSO)  $\delta$  8.30 (d,  $J = 7.7$  Hz, 2H), 7.03 (d,  $J = 7.8$  Hz, 2H), 4.15 (t,  $J = 7.2$  Hz, 2H), 3.18 (s, 6H), 1.80 – 1.67 (m, 2H), 1.29 – 1.15 (m, 6H), 0.85 (t,  $J = 7.0$  Hz, 3H).  $^{13}\text{C}$  NMR (151 MHz, DMSO)  $\delta$  155.79, 141.94, 129.48, 107.65, 56.66, 39.70, 30.58, 30.23, 25.05, 21.90, 13.82.



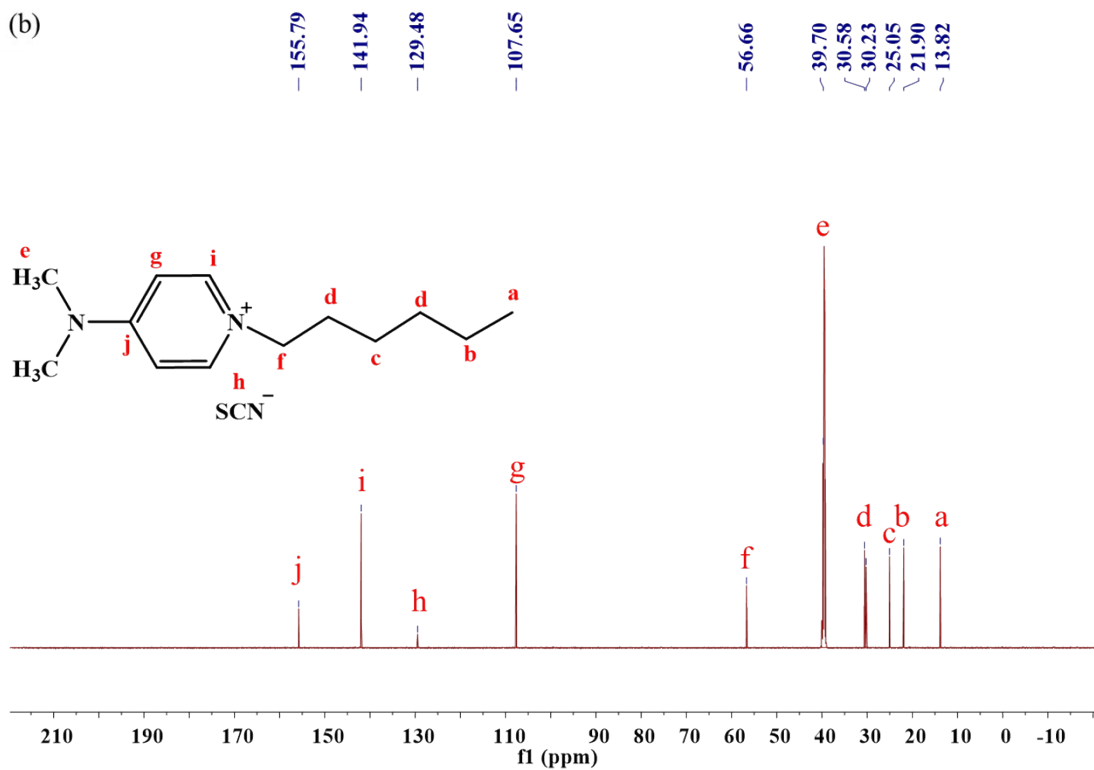


Figure S10.  $^1\text{H}$  NMR spectra (a) and  $^{13}\text{C}$  NMR spectra (b) of  $[\text{C}_6\text{DMAP}][\text{SCN}]$ .

$[\text{C}_8\text{DMAP}][\text{SCN}]$ :  $^1\text{H}$  NMR (600 MHz, DMSO)  $\delta$  8.31 (d,  $J = 7.8$  Hz, 2H), 7.04 (d,  $J = 7.8$  Hz, 2H), 4.16 (t,  $J = 7.2$  Hz, 2H), 3.19 (s, 6H), 1.89 – 1.60 (m, 2H), 1.32 – 1.12 (m, 10H), 0.82 (t,  $J = 7.0$  Hz, 3H).  $^{13}\text{C}$  NMR (151 MHz, DMSO)  $\delta$  155.75, 141.89, 129.57, 107.63, 56.66, 31.10, 39.67, 30.31, 28.47, 28.36, 25.39, 21.99, 13.87.

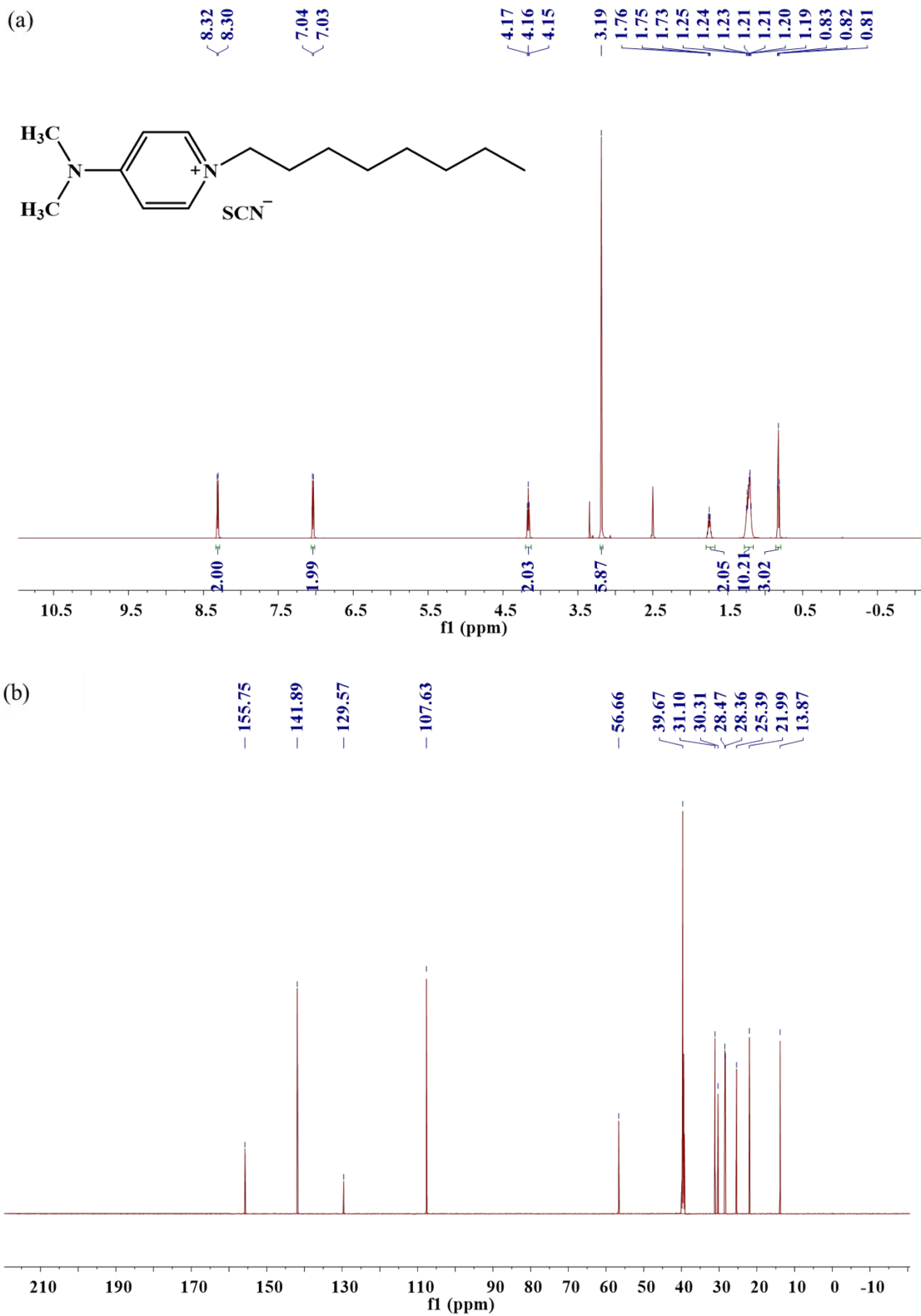


Figure S11.  $^1\text{H}$  NMR spectra (a) and  $^{13}\text{C}$  NMR spectra (b) of  $[\text{C}_8\text{DMAP}][\text{SCN}]$ .

$[\text{C}_{10}\text{DMAP}][\text{SCN}]$ :  $^1\text{H}$  NMR (600 MHz, DMSO)  $\delta$  8.31 (d,  $J = 7.8$  Hz, 2H), 7.04 (d,  $J = 7.8$  Hz, 2H), 4.16 (t,  $J = 7.2$  Hz, 2H), 3.19 (s, 6H), 1.80 – 1.66 (m, 2H), 1.28 –

1.15 (m, 14H), 0.83 (t,  $J = 7.0$  Hz, 3H).  $^{13}\text{C}$  NMR (151 MHz, DMSO)  $\delta$  155.76, 141.92, 129.54, 107.64, 56.66, 39.67, 31.24, 30.29, 28.84, 28.82, 28.61, 28.40, 25.39, 22.05, 13.90.

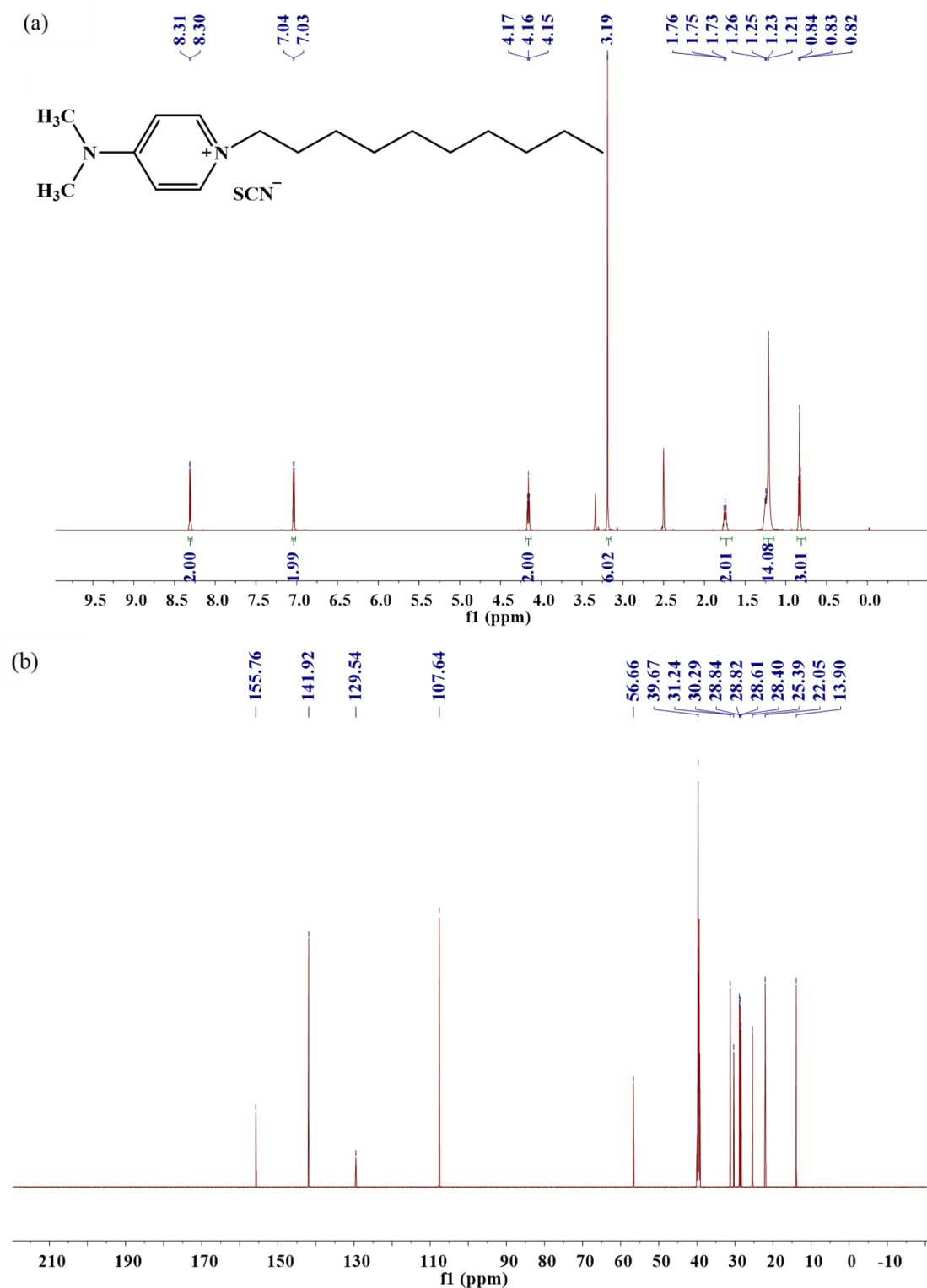
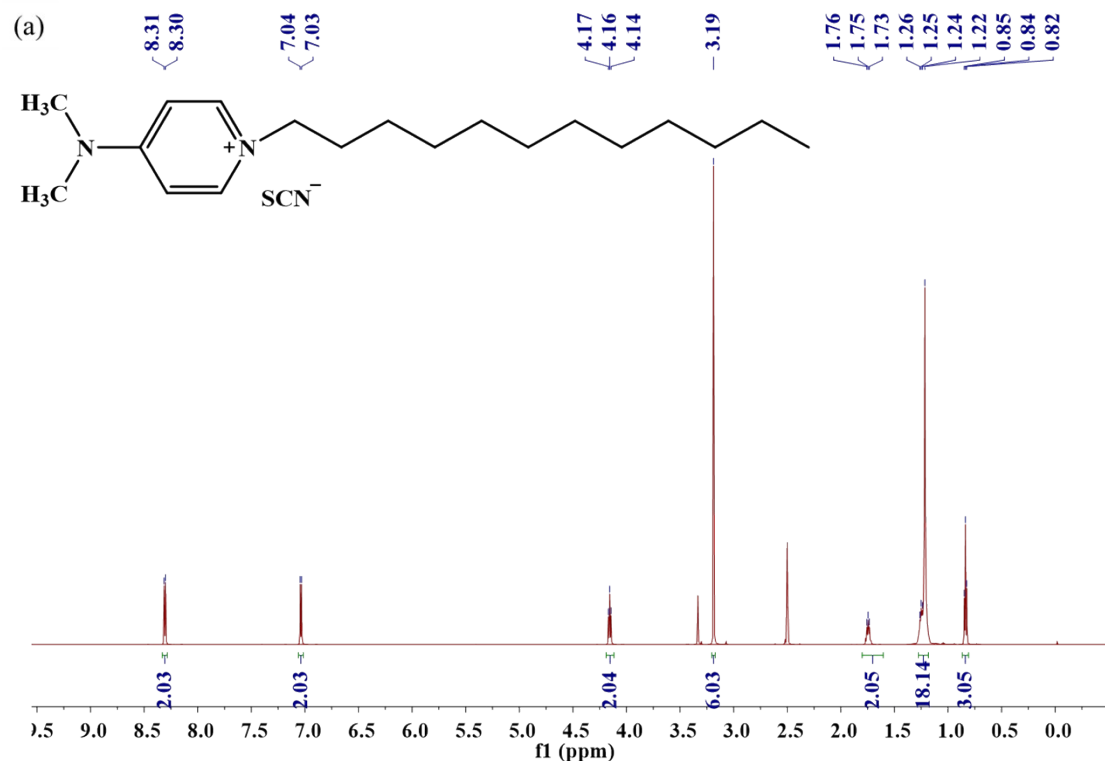


Figure S12.  $^1\text{H}$  NMR spectra (a) and  $^{13}\text{C}$  NMR spectra (b) of  $[\text{C}_{10}\text{DMAP}][\text{SCN}]$ .

[C<sub>12</sub>DMAP][SCN]: <sup>1</sup>H NMR (600 MHz, DMSO) δ 8.31 (d, *J* = 7.8 Hz, 2H), 7.04 (d, *J* = 7.8 Hz, 2H), 4.16 (t, *J* = 7.2 Hz, 2H), 3.19 (s, 6H), 1.80 – 1.60 (m, 2H), 1.28 – 1.18 (m, 18H), 0.84 (t, *J* = 7.0 Hz, 3H). <sup>13</sup>C NMR (151 MHz, DMSO) δ 155.77, 141.92, 129.53, 107.64, 56.66, 39.68, 31.27, 30.30, 28.98, 28.90, 28.83, 28.68, 28.41, 25.40, 22.06, 13.90.



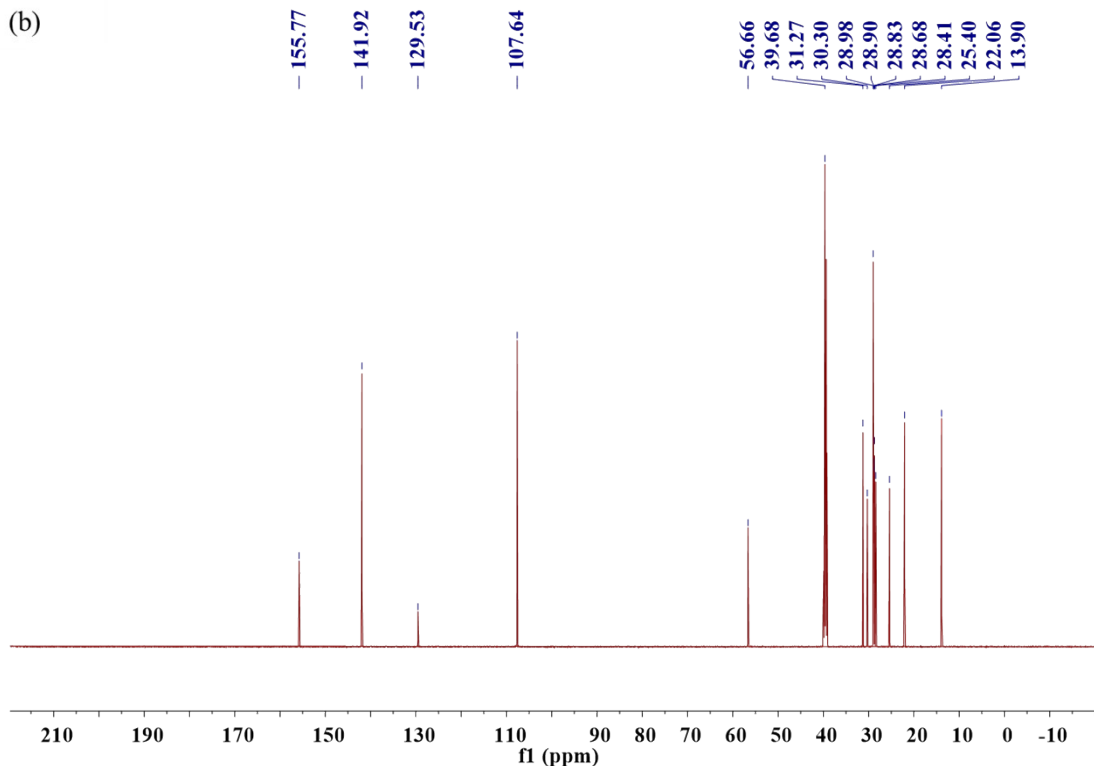


Figure S13.  $^1\text{H}$  NMR spectra (a) and  $^{13}\text{C}$  NMR spectra (b) of  $[\text{C}_{10}\text{DMAP}][\text{SCN}]$ .

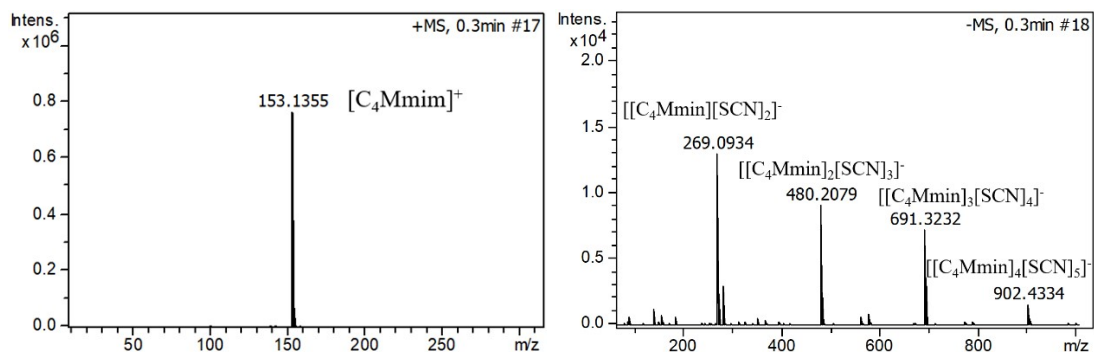


Figure S14. The ESI-MS spectrum of cation and anion modes of  $[\text{C}_4\text{Mmim}][\text{SCN}]$

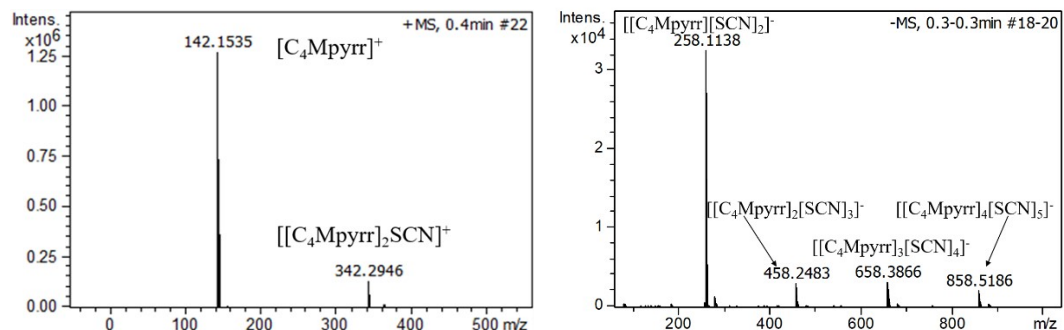


Figure S15. The ESI-MS spectrum of cation and anion modes of  $[\text{C}_4\text{Mpyrr}][\text{SCN}]$

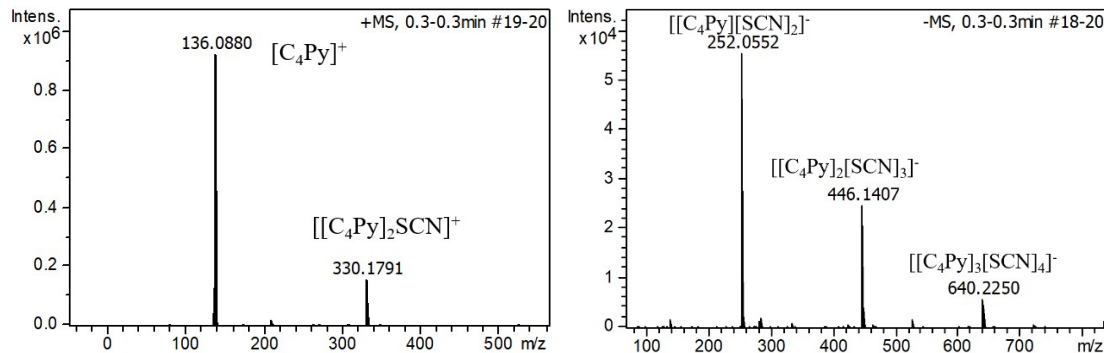


Figure S16. The ESI-MS spectrum of cation and anion modes of  $[\text{C}_4\text{Py}][\text{SCN}]$

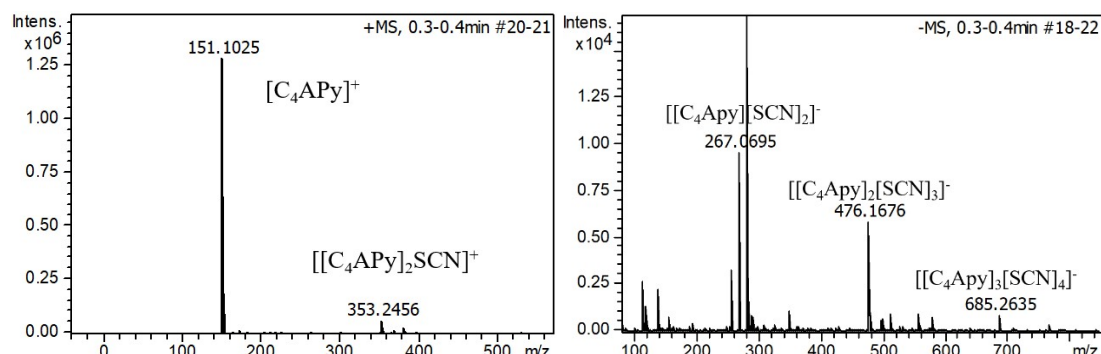


Figure S17. The ESI-MS spectrum of cation and anion modes of  $[\text{C}_4\text{APy}][\text{SCN}]$

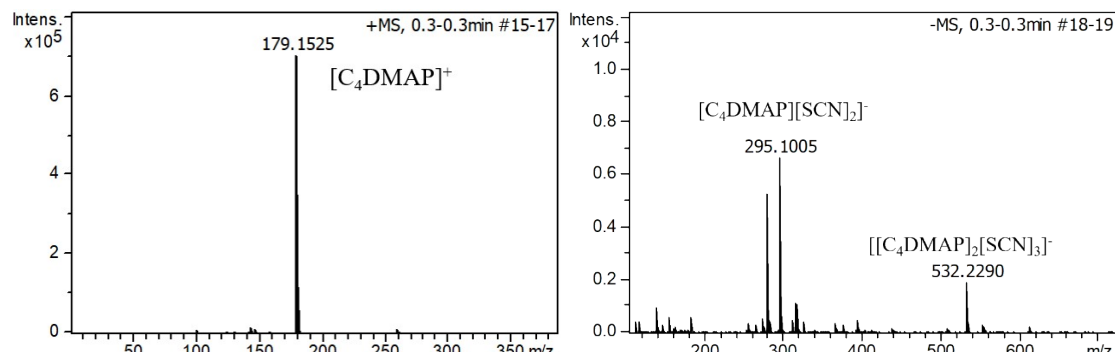


Figure S18. The ESI-MS spectrum of cation and anion modes of  $[\text{C}_4\text{DMAP}][\text{SCN}]$

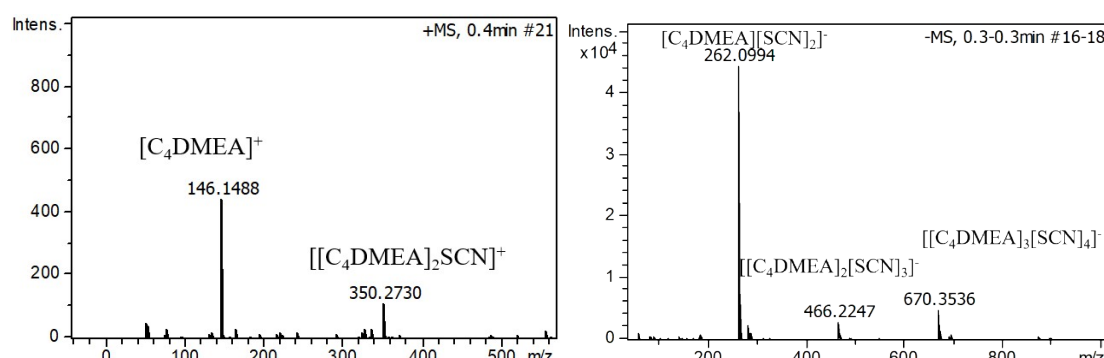


Figure S19. The ESI-MS spectrum of cation and anion modes of  $[\text{C}_4\text{DMEA}][\text{SCN}]$

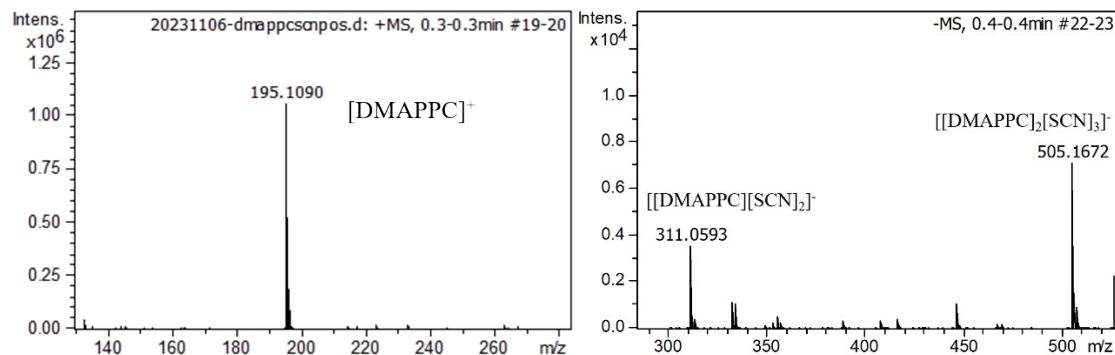


Figure S20. The ESI-MS spectrum of cation and anion modes of  $[\text{DMAPPC}][\text{SCN}]$

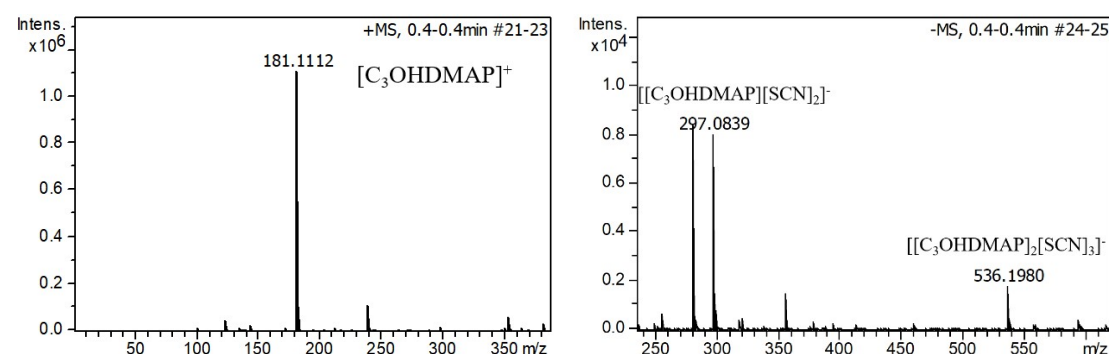


Figure S21. The ESI-MS spectrum of cation and anion modes of  $[\text{C}_3\text{OHDMAP}][\text{SCN}]$

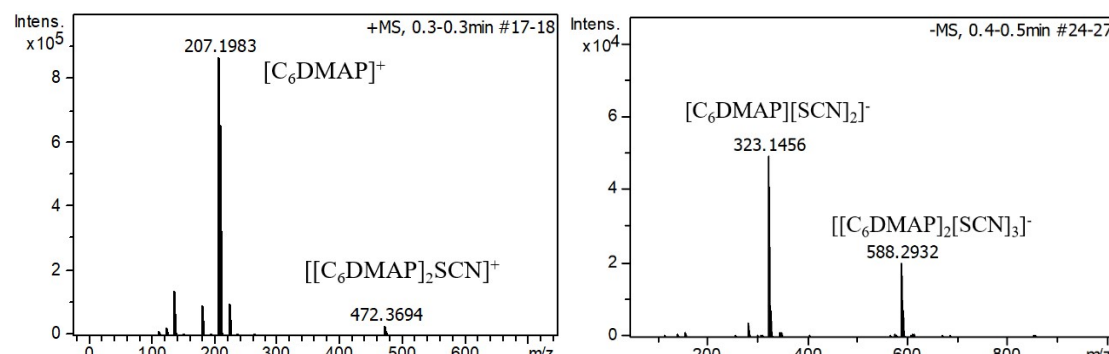


Figure S22. The ESI-MS spectrum of cation and anion modes of  $[\text{C}_6\text{DMAP}][\text{SCN}]$

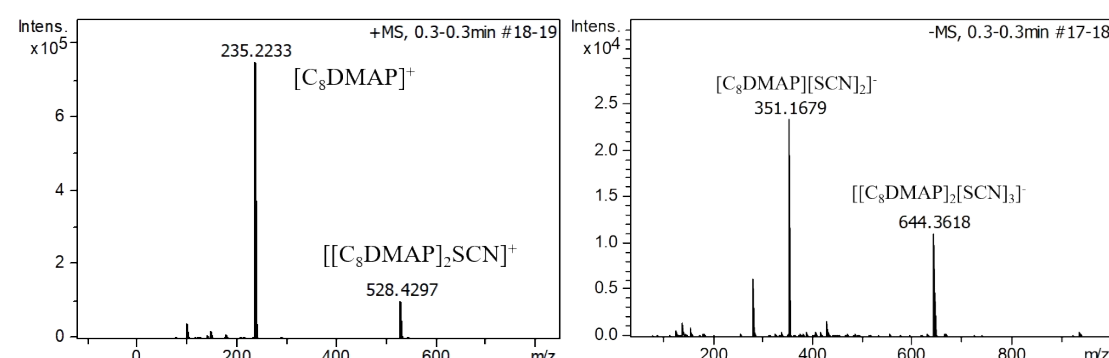


Figure S23. The ESI-MS spectrum of cation and anion modes of  $[\text{C}_8\text{DMAP}][\text{SCN}]$

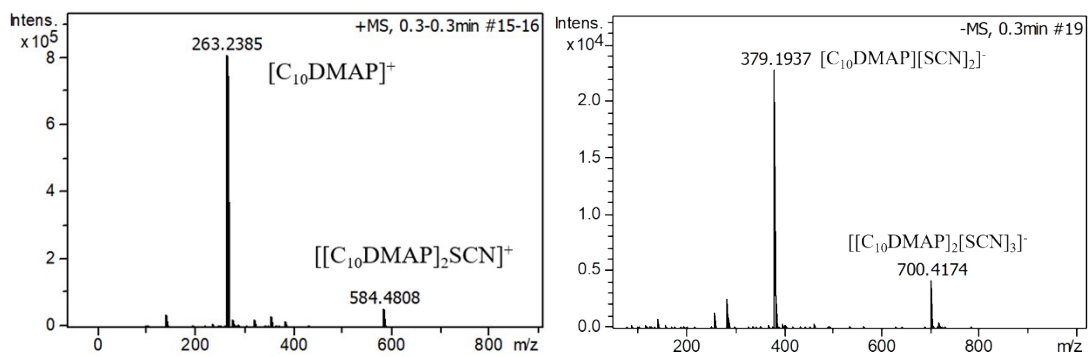


Figure S24. The ESI-MS spectrum of cation and anion modes of  $[\text{C}_{10}\text{DMAP}][\text{SCN}]$

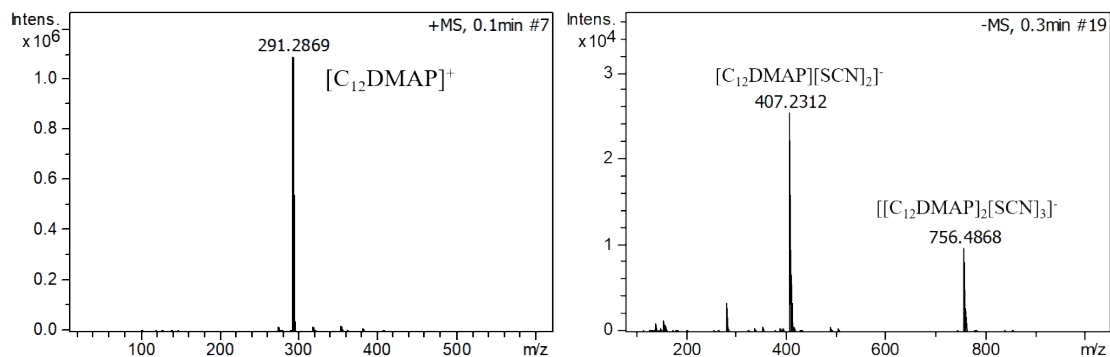


Figure S25. The ESI-MS spectrum of cation and anion modes of  $[\text{C}_{12}\text{DMAP}][\text{SCN}]$

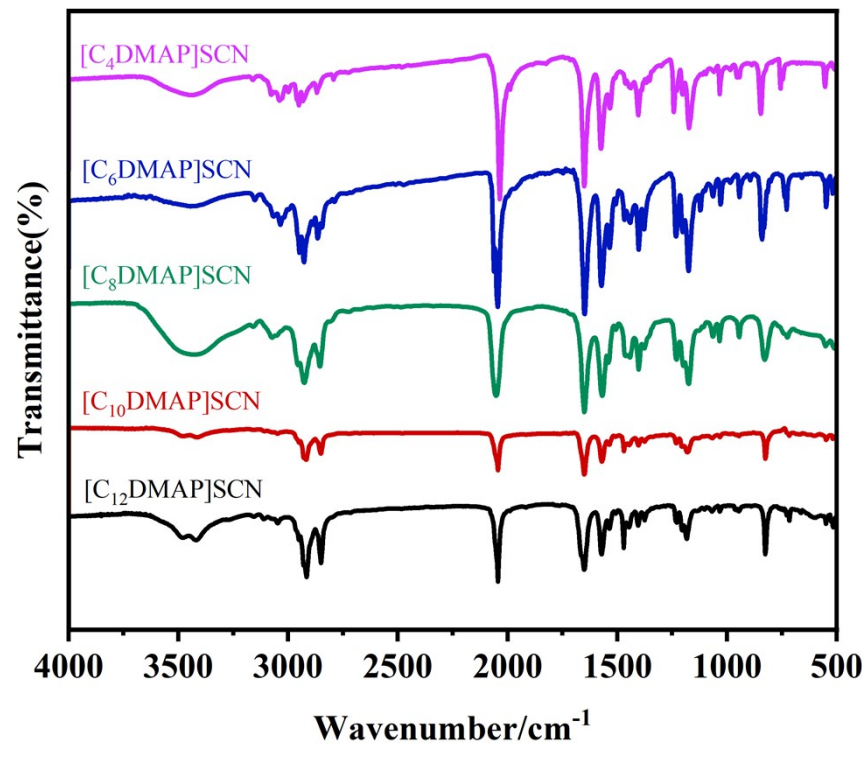


Figure S26. FT-IR spectra of DMAP-based thiocyanate ionic liquid

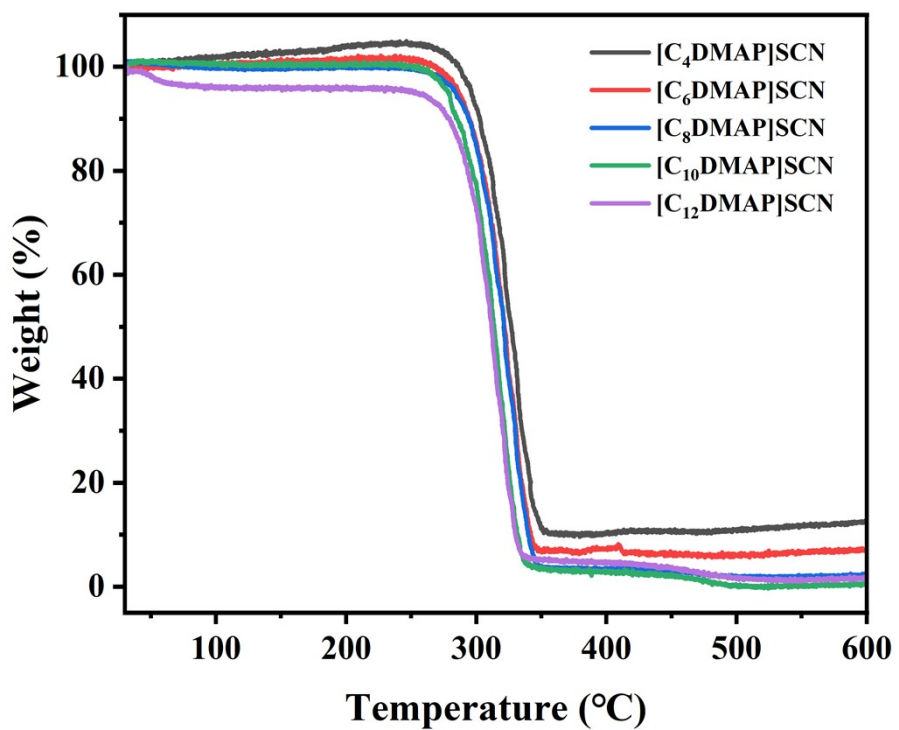


Figure S27. TGA curves of DMAP-based thiocyanate ionic liquid

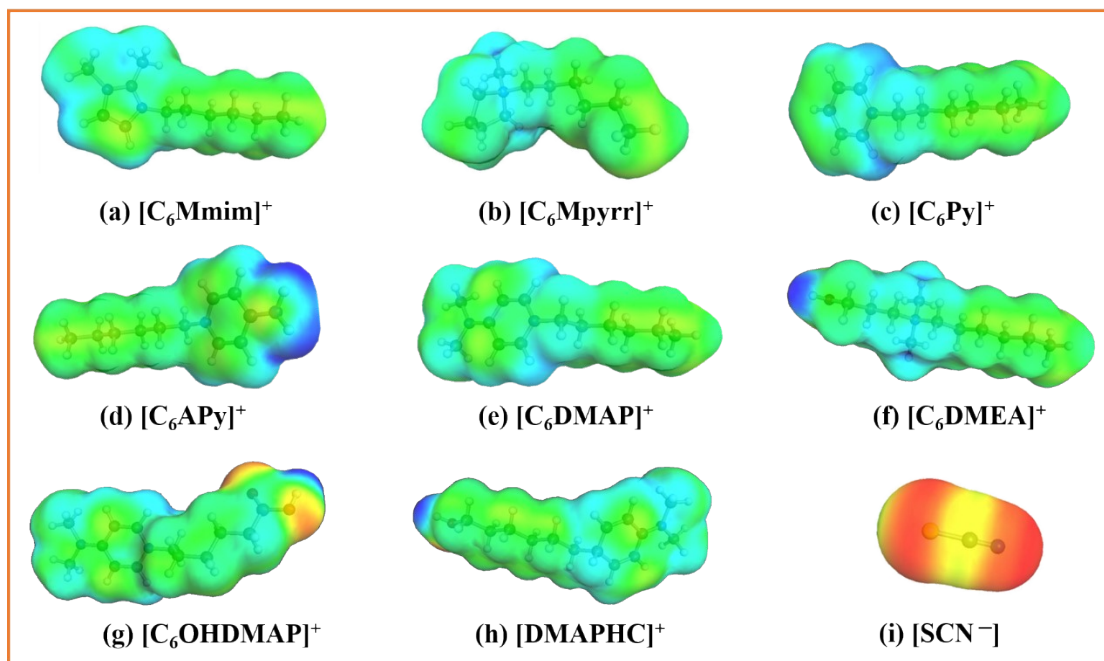


Figure S28. Cationic  $\sigma$ -surface (a-i) charge distribution of each ionic liquid. Red color = negative surface charge (high electron density, nucleophilic region), blue = positive surface charge (low electron density, electrophilic region), green and yellow indicate relatively neutral charges.)

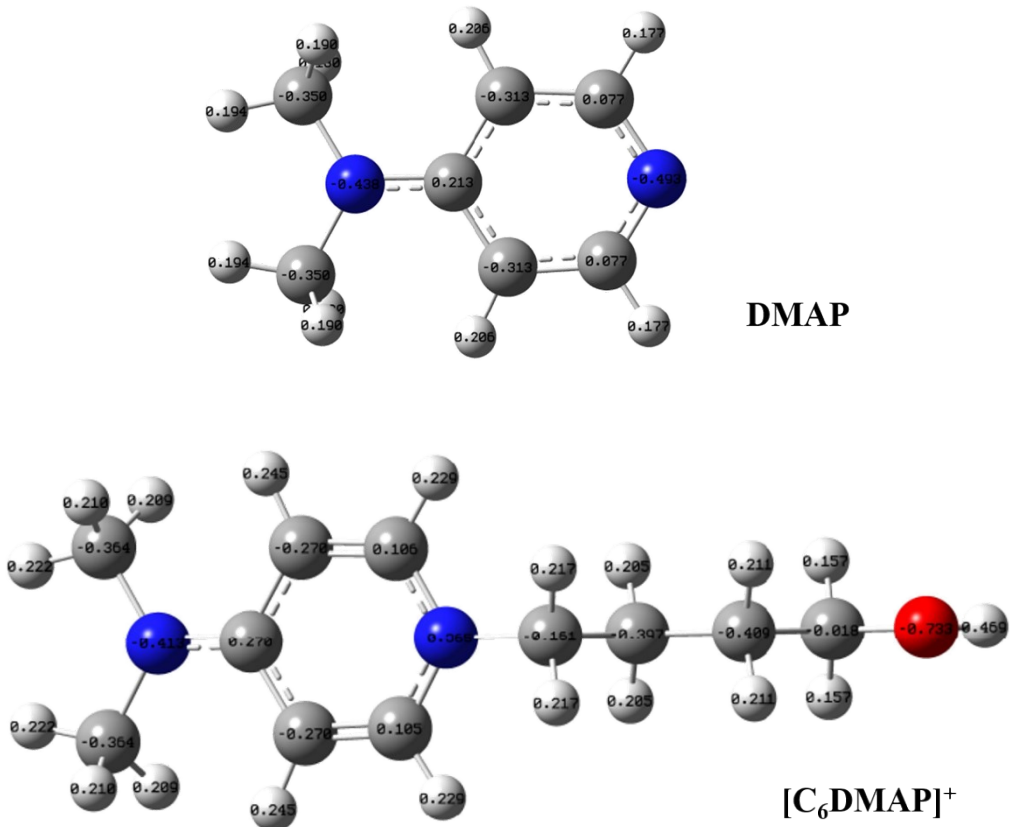


Figure S29. NBO charge distribution of the DMAP and [C<sub>6</sub>DMAP][SCN]structure